



# Responses of Primary Afferent Fibers to Acupuncture-Like Peripheral Stimulation at Different Frequencies: Characterization by Single-Unit Recording in Rats

Ran Huo<sup>1,2,3,4</sup> · Song-Ping Han<sup>1,2,3</sup> · Feng-Yu Liu<sup>1,2,3</sup> · Xiao-Jing Shou<sup>1,2,3</sup> ·  
Ling-Yu Liu<sup>1,2,3</sup> · Tian-Jia Song<sup>1,2,3</sup> · Fu-Jun Zhai<sup>1,2,3</sup> · Rong Zhang<sup>1,2,3,5</sup> ·  
Guo-Gang Xing<sup>1,2,3,5</sup> · Ji-Sheng Han<sup>1,2,3</sup>

Received: 16 June 2019 / Accepted: 18 January 2020 / Published online: 11 May 2020  
© Shanghai Institutes for Biological Sciences, CAS 2020

**Abstract** The pain-relieving effect of acupuncture is known to involve primary afferent nerves (PANs) *via* their roles in signal transmission to the CNS. Using single-unit recording in rats, we characterized the generation and transmission of electrical signals in A $\beta$  and A $\delta$  fibers induced by acupuncture-like stimuli. Acupuncture-like signals were elicited in PANs using three techniques: manual acupuncture (MAc), emulated acupuncture (EA<sub>c</sub>), and electro-acupuncture (EA)-like peripheral electrical stimulation (PES). The discharges evoked by MAc and EA<sub>c</sub> were mostly in a burst pattern with average intra-burst and inter-burst firing rates of 90 Hz and 2 Hz, respectively. The frequency of discharges in PANs was correlated with

the frequency of PES. The highest discharge frequency was 246 Hz in A $\beta$  fibers and 180 Hz in A $\delta$  fibers. Therefore, EA in a dense-disperse mode (at alternating frequency between 2 Hz and 15 Hz or between 2 Hz and 100 Hz) best mimics MAc. Frequencies of EA output >250 Hz appear to be obsolete for pain relief.

**Keywords** Acupuncture · Peripheral electrical stimulation · Dorsal root · Primary afferent fiber · Electrophysiology · Single unit recording

## Introduction

As an important technique in Traditional Chinese Medicine, acupuncture may be the most frequently used alternative and complimentary technique world-wide due to its prominent therapeutic effects. However, the consistency and reproducibility of these effects need further improvement. A better understanding of the mechanisms underlying the current technology and concepts is critical to making this thousand-year old technique more effective. We designed the present study to explore the production, processing, and transmission of acupuncture-like signals from the periphery to the CNS where various neurotransmitters and neuropeptides are released to activate descending analgesic pathways [2, 12, 14].

Manipulation techniques such as lifting, inserting, and twisting are considered to be critical in acupuncture therapy [4, 7]. Previous studies have shown that various manipulation styles produce distinctive patterns of brain activity [1, 8, 18, 26, 28]. Three techniques were used in the present study to elicit acupuncture-like signals: manual acupuncture (MAc), electro-acupuncture (EA), and EA-like peripheral electrical stimulation (PES).

Ran Huo and Song-Ping Han have contributed equally to this work.

**Electronic supplementary material** The online version of this article (<https://doi.org/10.1007/s12264-020-00509-3>) contains supplementary material, which is available to authorized users.

✉ Guo-Gang Xing  
gging@bjmu.edu.cn

✉ Ji-Sheng Han  
hanjisheng@bjmu.edu.cn

- <sup>1</sup> Neuroscience Research Institute, Peking University, Beijing 100191, China
- <sup>2</sup> Department of Neurobiology, Peking University School of Basic Medical Sciences, Beijing 100191, China
- <sup>3</sup> Key Laboratory for Neuroscience, Ministry of Education/National Health and Family Planning Commission, Peking University, Beijing 100191, China
- <sup>4</sup> Department of Radiology, Peking University Third Hospital, Beijing 100191, China
- <sup>5</sup> Department of Integration of Chinese and Western Medicine, Peking University School of Basic Medical Sciences, Beijing 100191, China

It has been shown that the discharge activity in the sciatic nerve tract, a fine nerve bundle in the spinal dorsal root, and wide dynamic range neurons, is elevated in response to MAC or EA applied to the Zusanli acupoint (ST36) in the leg [16, 25, 36]. However, compound action potentials recorded in a nerve bundle do not permit the characterization and analysis of activity in an individual afferent fiber. Using single-unit recording from the dorsal root (DR) of lumbar segments 4 and 5 (L4/5), we set out to determine how acupuncture-induced electrical signals in primary fibers (acupuncture signals) are transmitted from the terminals of PANs to the CNS.

It is controversial as to which type of PAN is involved in transmitting acupuncture signals to the CNS. In the present work, we focused on A $\beta$  and A $\delta$  fibers since we have shown that they are the most important types of PAN in transmitting the acupuncture signal at least in the context of antinociception. Some investigators have shown that all the four populations of afferent fibers, including C-fibers, are activated by acupuncture-like stimulation [19, 20, 37]; however, the C-fiber activation usually requires very strong stimulation and is accompanied by an uncomfortable sensation.

An important finding in our previous studies of EA therapy was the frequency-dependence, which might be more critical than any other parameters. For example, the types of opioid peptides released and the analgesic effect produced by EA are all frequency-dependent [11]. Low (2 Hz)- and high (100 Hz)-frequency EA activates different neural pathways, releases different endorphins, causes binding to different receptors, and has different therapeutic effects [13, 15, 32, 33]. However, information is limited on how the signal is produced and processed in PANs by acupuncture-like stimulation at various frequencies. This information is critical in our efforts to further optimize EA parameters.

In the present study, we set out to accomplish three goals: (1) to characterize the firing patterns in A $\beta$ - and A $\delta$ -fibers in response to various forms of mechanical stimulation at the ST36 acupoint; (2) to explore how PES signals at the optimal frequency, pulse-width, and intensity are processed in PAN fibers; and (3) to assess the conduction efficiency of PAN fibers in response to PES over the whole range of clinically-relevant frequencies (100 Hz–1000 Hz).

## Materials and Methods

### Animals

Male Sprague-Dawley rats weighing 250 g–350 g were obtained from the Department of Experimental Animal Sciences, Peking University Health Science Center. They were housed no more than 4 per cage and maintained on artificial light 07:00–19:00 day/night cycles at a room

temperature of 20°C–25°C, 50% relative humidity, and food and water freely available. All the animal experimental procedures were in line with the National Institutes of Health Guide for the Care and Use of Laboratory Animals, and were approved by Peking University Animal Use and Care Committee.

## Neurophysiological Experiments

### Single-Unit Recording

Each rat was anesthetized with urethane (1.4 g/kg, i.p.) and maintained with supplemental doses as needed. A tracheostomy was performed to keep the airway unobstructed. The left external jugular vein was cannulated for the slow administration of fluids and the arterial O<sub>2</sub> saturation was maintained at >90%. Heart rate (375 bpm–450 bpm) was monitored by a small animal vital signs monitor. Rectal temperature was maintained at 36.5°C–37.5°C throughout the experiments with cotton under the body and a heating lightbulb overhead. The pupil size, corneal reflex, skin color, and skeletal muscle reflexes were closely monitored during experiments. An experiment would be terminated if these physiological indicators appeared abnormal.

The erector spinae was separated from both sides of the spinous process and partially resected. In the prone position, a lumbosacral laminectomy was performed to expose the L4/5 DR. The roots were covered with warm paraffin oil at 37°C in a pool formed by skin flaps. The temperature of the paraffin oil was maintained at 36.5°C–37.5°C to avoid the influence of temperature on nerve fiber conduction velocity (CV).

The DR of the L4/5 spinal nerve on the left side was cut close to its entry into the spinal cord, teased from the DR using fine forceps, and mounted on a platinum wire electrode (0.2 mm in diameter) for recording, with the reference electrode connected to nearby tissue (Fig. 1A). Only nerve bundles without spontaneous activity or evoked firing by applying brush to the skin were further studied. Most of the data were collected from the L5 spinal nerve and a small proportion from the L4 spinal nerve; we pooled the two together for analysis. Data were captured and analyzed using Micro 1401 mk II coupled to a Pentium computer with Spike2 software (Cambridge Electronic Design, Cambridge, UK). Only neural signals with signal-to-noise ratios >1.5 were accepted for further analysis.

### Measurement of Conduction Velocity of Single-Unit Afferent Fibers

In some of the PES experiments, the peripheral receptive located on the glabrous skin of the hind paw was identified

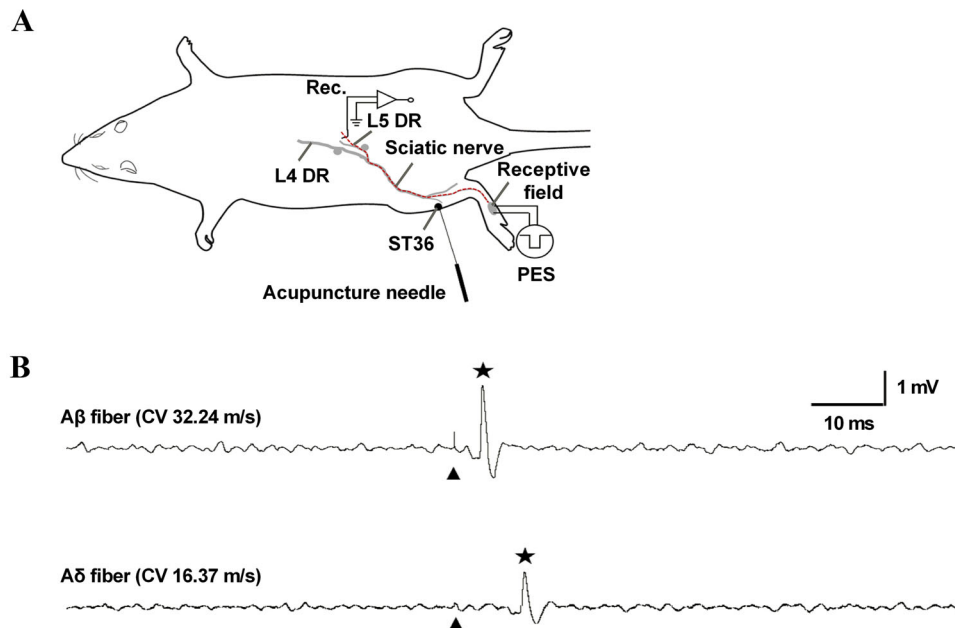


**Fig. 1** Experimental setup for *in vivo* single-unit recording in the L4/5 DR. **A** Recording site on the left L4/5 DR and stimulating site at the ipsilateral ST36 (for MAC or EAc) or in the corresponding receptive field (for PES). **B** Example traces of evoked discharges (indicated by a star) recorded in an A $\beta$ -fiber (conduction distance, 113 mm; latency, 3.30 ms; CV, 34.24 m/s) and an A $\delta$ -fiber (conduction distance, 131 mm; latency, 8.00 ms; CV, 16.37 m/s) following a single square-wave

stimulus applied to the corresponding receptive field. The single stimulus intensity (artifacts indicated by arrowheads) was 1.5 times the threshold of the afferent fiber. L4/5 DR, lumbar 4 or 5 dorsal root; ST36, Zusanli acupoint; MAC, manual acupuncture; EAc, emulation acupuncture PES, peripheral electrical stimulation; CV, conduction velocity.

using von Frey hairs after the target single-unit afferent fiber was identified. After locating the most sensitive point in the receptive field of the single-unit afferent fiber, the latency of the evoked discharge in the dissected dorsal root fiber was measured by stimulation with a negative square-wave (100  $\mu$ s pulse width for A $\beta$  fibers and 500  $\mu$ s for A $\delta$  fibers) at 1.5 times the threshold current delivered by a pair of electrodes inserted under the skin in parallel and centripetally (Fig. 1A) [5]. The CV of each afferent fiber was calculated as the distance between the stimulating and recording electrodes divided by the latency of the evoked discharge. Based on CV (without temperature correction), target fibers were classified as myelinated A $\beta$  fibers (CV, 25 m/s–72 m/s) or thin myelinated A $\delta$  fibers (CV, 2 m/s–24 m/s) (Fig. 1B) [17, 21].

## Experimental Protocols

### *MAC and Emulated Acupuncture (EAc) at Human ST36 in Rats*

After the hair of the left hind limb was shaved and before teasing out the single-unit fiber, a stainless-steel acupuncture needle (0.25 mm in diameter) was inserted into the site equivalent to human ST36 (5 mm lateral to the anterior tubercle of the tibia) (Fig. 1A). A rubber plug on the needle

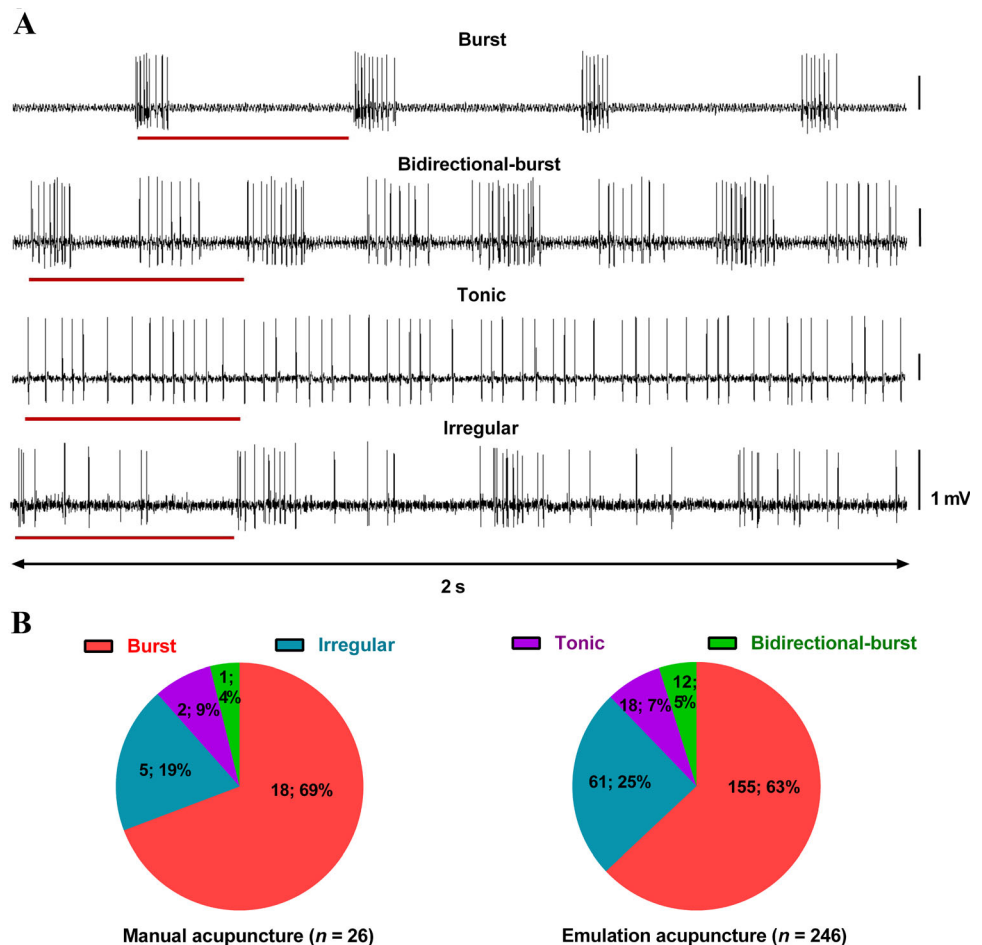
was positioned 7 mm from the tip to standardize the depth of insertion. Fiber types were not identified in these experiments.

In MAC, a target single-unit afferent fiber was identified if evoked discharges were recorded during MAC around ST36. Evoked discharges of the target fiber were continuously recorded when the acupuncture needle was twisted manually at a frequency of once or twice per second for 60 s (Fig. 2A).

Due to the high variation and low reproducibility of the needle manipulation parameters in MAC, a novel EAc apparatus (ZSF-I) was developed at Shanghai University of Traditional Chinese Medicine. The twirling angle (90°, 180°, or 360°) and number of times per second of needle twisting (one, two, or three times per second) can be set in any combination. A uniform speed of rotation was maintained during most of the time in one cycle of needle manipulation. The range of lifting and inserting the needle (up and down movement of the needle) was 3 mm to a maximum depth of 7 mm. The evoked discharges in the target fiber in response to EAc around ST36 were continuously recorded with various combinations of twirling angle and times per second of twisting in 60 s.

Data were collected with the aid of Spike2 software, and the firing rates and patterns of evoked discharges were analyzed off-line.

**Fig. 2** Patterns of evoked discharges in single-unit afferent fibers of the L4/5 DR in response to MAc and EAc at ST36. **A** Representative traces of the four discharge patterns of single-units in response to MAc and EAc. The lines below traces represent one cycle of needle twisting (One time per second). **B** Distribution of the four types of discharge following MAc and EAc stimulation (number of recorded fibers; percentage). Note that the distributions are similar following MAc and EAc stimulation. L4/5 DR, lumbar 4 or 5 dorsal root; MAc, manual acupuncture; EAc, emulated acupuncture; ST36, Zusanli acupoint.



### PES at Frequencies not Exceeding 100 Hz Delivered to the Receptive Fields of Afferent Fibers

Single-unit activity was recorded from a fiber in the dorsal root of the L4/5 spinal nerve on the left side when PES was delivered to its receptive field after measuring the latency of its evoked discharge. A pair of stimulating electrodes were connected to a constant-current stimulator (HANS-200A, Nanjing Jesen Co., Nanjing, China) (Fig. 1A). Alternating positive and negative rectangular square-wave pulses were delivered at various frequencies including single frequency (2 Hz, 15 Hz, and 100 Hz) and alternating frequency, also called a dense-disperse mode (EA or PES at alternating frequency between 2 Hz and 15 Hz [2/15 Hz] for 3 s each, or between 2 Hz and 100 Hz [2/100 Hz] for 3 s each) (Table 1). When the stimulation threshold of a target single-unit afferent fiber had been identified and then the current gradually increased, the responses to PES at the above frequencies were recorded. The activity of the target fiber was recorded continuously for 30 min during PES (intensity: 1–2 times the threshold current) at randomly-selected frequencies ( $\leq 100$  Hz). Data were analyzed using spike2 software. The response ratio was calculated as the

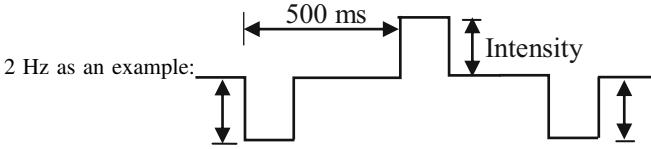
ratio of the number of evoked discharges to the number of electrical stimuli delivered multiplied by 100.

### PES at Frequencies Up to 1000 Hz Delivered to the Receptive Fields of Afferent Fibers in Rats

In these experiments, 100-Hz PES (negative square wave, pulse width, 100  $\mu$ s; intensity,  $2\times$  threshold current) delivered to the receptive field for 60 s served as the positive control. Only single-unit afferent fibers with a 100% response ratio following PES at 100 Hz were studied further.

The activity of single units in response to PES (parameters as above) delivered to the receptive field at random frequencies (100 Hz, 200 Hz, 300 Hz, 400 Hz, 500 Hz, 600 Hz, 700 Hz, 800 Hz, 900 Hz, and 1000 Hz) was recorded continuously for 60 s. If the response ratio at any frequency was  $<100\%$ , the results were validated by the presence of a normal response (response ratio, 100%) to PES at 100 Hz after the fiber was allowed to rest for 5 min. This procedure helped to exclude the artifact that the reduced response ratio was due to neuronal damage rather than the PES frequency exceeding the transduction capacity (i.e. the refractory period) of the fiber.

**Table 1** Parameters of the HANS-200A stimulator.

Frequency (Hz)	Pulse Width ( $\mu$ s)	Wave-form
2	600	
15	400	
100	200	
2/15	Alternating 2 Hz and 15 Hz for 3 s each	
2/100	Alternating 2 Hz and 100 Hz for 3 s each	

The data were collected and analyzed using the method described for PES at frequencies not exceeding 100 Hz.

## Data Analysis

Statistical analysis was performed using SPSS ver. 19 (IBM Inc., Chicago, IL) and graphs were generated using Prism 6.0 (GraphPad Software Inc., San Diego, CA). Data from some of the EAc experiments were analyzed using non-parametric tests (Kruskal–Wallis test followed by Dunn’s multiple comparisons test) and are presented as the median  $\pm$  interquartile range for a non-normal distribution. Comparisons of response ratio–stimulus frequency between A $\beta$  and A $\delta$  fibers were analyzed by repeated measures ANOVA. Other comparisons between or among different groups used the unpaired *t* test or one-way ANOVA and values are expressed as the mean  $\pm$  SEM unless otherwise specified. Differences with *P* values  $<0.05$  (two-tailed) were considered significant.

## Results

### Characterization of Evoked Discharges in PAN Fibers by Mechanical Stimulation at Acupoint ST36

#### Characteristics of the Patterns of Evoked Discharges

All single-unit afferent fibers recorded in the present study were silent with no spontaneous discharges in the absence of mechanical acupuncture stimulation. The results showed four distinct firing patterns of discharge in fibers in response to MAc and/or EAc, summarized as follows (Fig. 2A, B):

1. **Burst firing:** recurring, abrupt discharges when the needle was rotated clockwise. There was no evoked discharge during anticlockwise rotation. This pattern was most common under all experimental conditions, accounting for 69% with MAc and 63% with EAc. Note that almost all the burst firing occurred when the needle was rotated to near its maximum angle (90°, 180°, or 360°).
2. **Bidirectional-burst firing:** burst firing when the needle was rotated both clockwise and anticlockwise. They made up 4% during MAc and 5% during EAc.
3. **Tonic firing:** a continuous and irregular pattern during needle manipulation. There was no clear difference among the inter-spike intervals (ISIs) of evoked discharges of a fiber. They constituted  $\sim 9\%$  in MAc and  $\sim 7\%$  in EAc.
4. **Irregular firing:** no particular pattern. All firing was included in this category except for the three types above. Again, more evoked discharges occurred when the needle was rotated clockwise than anticlockwise. They made up 19% in MAc and 25% in EAc.

### Activity Level (Number of Evoked Spikes per Second) of PAN Fibers

Single-unit afferent fibers of the L4/5 spinal dorsal root in rats were activated by acupuncture-like mechanical stimulation at ST36. Only initially silent afferent bundles were examined in order to eliminate interference from spontaneous discharges.

In MAc, the discharge activity of 26 bundles from 11 rats was randomly divided into two groups: a one twist per second group ( $n = 12$ ) and a two twists per second group ( $n = 14$ ). There were more evoked spikes in the two-twists than in the one-twist group ( $7.7 \pm 0.8$  spikes/s vs  $14.9 \pm 1.5$  spikes/s,  $P < 0.001$ , unpaired *t* test; Fig. 3A(a), B).

In the EAc experiments, the needle was inserted into the ST36 acupoint. In order to quantify the effects of various manipulation styles on discharge activity in PAN fibers, the needle rotation angle was preset to 90°, 180°, or 360°. At each rotation angle, the number of twists per second was delivered once, twice, or three times.

In the 90° EAc group, 84 bundles were recorded from 21 rats, and they were randomized into three groups with one, two, or three twists per second ( $n = 28, 27,$  and  $29$ , respectively). The numbers of evoked spikes increased with the number of twists per second and the medians were 8.05, 14.80, and 20.00, respectively (Fig. 3A(b), C).

In the 180° EAc study, 81 bundles (28, 27, and 26 per group) were recorded from 22 rats, and in the 360° EAc study, 81 bundles (26, 28, and 27 per group) were recorded from 19 rats. Similar increases were found in the

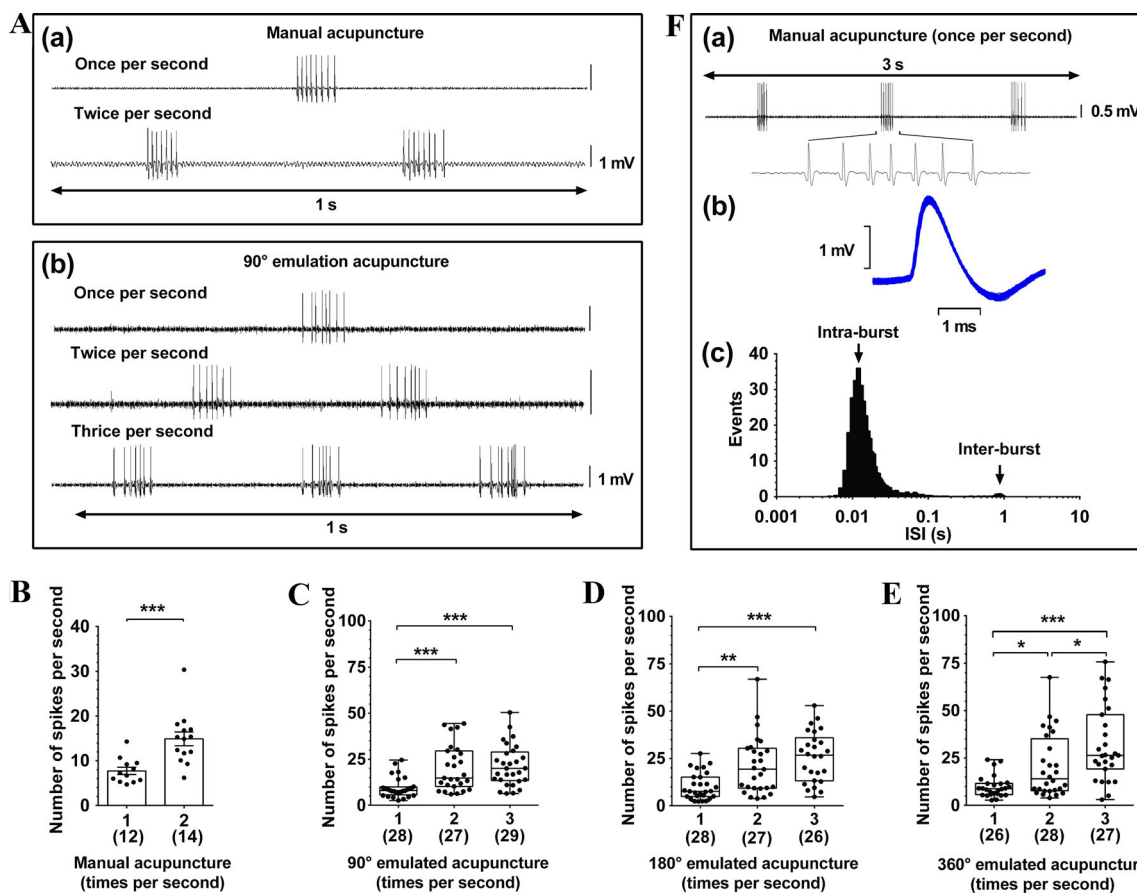


**Fig. 3** Evoked discharges of single-unit afferent fibers in the L4/5 dorsal root in response to MAC and EAc at ST36. **A** Representative recordings from fibers in response to MAC and EAc at an angle of 90°. **B–E** More discharges were evoked with increasing numbers of twists per second with MAC (**B**) and EAc (**C–E**). **F** Representative recordings and ISI histogram of evoked burst firing in the same fiber in response to MAC (once/second). **(a)** Three-second recording during MAC. **(b)** Superimposed wavelet plot of all the evoked discharges in the fiber shown in **A** during MAC for 60 s (once per second). **(c)** ISI

distribution within a burst (0.01 s–0.02 s, arrow) and between bursts (~1 s, arrow) (binwidth, 1 ms; a log scale (abscissa) was used to show all intervals). Data are expressed as the mean  $\pm$  SEM (**B**, unpaired *t* test) or median and 25–75th percentiles (**C–E**, outliers beyond the 1.5 interquartile ranges were removed, non-parametric tests). Digits in brackets are the number of fibers. \* $P < 0.05$ , \*\* $P < 0.01$ , and \*\*\* $P < 0.001$ . ISI, inter-spike interval; MAC, manual acupuncture; EAc, emulated acupuncture; ST36, Zusanli acupoint.

180° (median, 7.65, 19.30, and 26.75;  $P < 0.01$  or  $P < 0.001$ , Kruskal-Wallis test followed by Dunn's multiple comparisons test; Fig. 3D) and 360° groups (median, 8.75, 14.00, and 26.40;  $P < 0.05$  or  $P < 0.001$ , test as for 180°; Fig. 3E).

There were no significant differences in the numbers of evoked spikes per second between the EAc groups with 90°, 180°, or 360° rotation (Fig. S1).

These data suggest that the number of times per second in a certain range of manipulating the needle is the most important factor affecting the level of the evoked response (spikes per second) to mechanical acupuncture. Furthermore, these data suggest that increases in the rotation angle of the needle under experimental conditions do not result in a higher level of activation of the afferent fibers in response to mechanical acupuncture.

### ISIs of Evoked Discharges of PAN Fibers During MAC at Once per Second

Having demonstrated above that burst firing (Fig. 2B) was the most common pattern of evoked discharges in response to MAC at once per second, and given that MAC is used widely in clinical settings, we next focused on characterizing the firing pattern in MAC at once per second.

Twelve single-unit afferent fibers (11 burst firing and 1 irregular firing) were recorded from 5 rats in response to MAC at once per second. We examined the ISIs of evoked discharges of target fibers to explore the discharge distribution. Typical fiber recordings showed that the ISIs within a burst ranged from 0.01 s to 0.02 s. The mean frequency of evoked discharges within a burst was between 50 Hz and 100 Hz (frequency = 1/ISI) with a peak at 83 Hz (Fig. 3F).

Considering the limited number of non-bursting fibers, we focused the ISI analysis on burst firing (11 fibers). The results revealed that the evoked discharges could be further classified into two categories: burst firing and sporadic firing (Fig. 4A). A burst was defined by the following criteria: (1) a maximum ISI within a burst  $\leq 0.019$  s; (2) an ISI between bursts  $> 0.1$  s; and (3)  $\geq 3$  spikes per burst. Among the 11 bursting fibers, most of the ISIs were  $< 0.02$  s with a peak at 0.012 s and a minimum of 0.005 s (Fig. 4B). The results showed that the number of intra-burst spikes was  $5.55 \pm 0.43$  (mean  $\pm$  SEM), the frequency of evoked intra-burst discharges was  $89.77$  Hz  $\pm 2.08$  Hz, and the frequency of evoked inter-burst discharges was  $2.36$  Hz  $\pm 0.30$  Hz (Fig. 4C).

### PES at Frequencies not Exceeding 100 Hz Delivered to the Receptive Fields of PAN Fibers

A total of 72 A $\beta$  fibers were recorded from 21 rats and randomized into 2-Hz ( $n = 14$ ), 15-Hz ( $n = 14$ ), 2/15-Hz ( $n = 15$ ), 100-Hz ( $n = 15$ ), and 2/100-Hz groups ( $n = 14$ ) (Fig. 5A). For A $\delta$  fibers, 67 bundles were recorded from 32 rats with 14, 12, 13, 16, and 12 bundles in each of the frequency groups as described for A $\beta$  fibers. The response ratio was used to describe the responses of neurons to a series of stimuli, and showed no significant differences between A $\beta$  fibers and A $\delta$  fibers in the response ratio to

PES at each of the frequencies, at least in the initial 60 s of simulation (A $\beta$ :  $100\% \pm 0\%$ ,  $100\% \pm 0\%$ ,  $99.48\% \pm 0.52\%$ ,  $99.27\% \pm 0.73\%$ , and  $99.44\% \pm 0.57\%$ ; A $\delta$ :  $100\% \pm 0\%$ ,  $100\% \pm 0\%$ ,  $100\% \pm 0\%$ ,  $97.83\% \pm 1.51\%$ , and  $100\% \pm 0\%$ ; one-way ANOVA; Fig. 5B, C). Similarly, in studies with a longer stimulation/recording period (30 min), A $\beta$  fibers retained an almost 100% response ratio during PES at the various specified frequencies ( $97.49\% \pm 2.50\%$ ,  $97.85\% \pm 1.65\%$ ,  $99.61\% \pm 0.39\%$ ,  $93.43\% \pm 2.93\%$ , and  $93.21\% \pm 3.25\%$ ; one-way ANOVA; Fig. 5D). In contrast, the response ratio in A $\delta$  fibers following 100-Hz PES was only  $80.17\% \pm 6.11\%$ , significantly lower than that in response to other frequencies (2 Hz,  $100\% \pm 0\%$ ; 15 Hz,  $97.99\% \pm 2.01\%$ ; 2/15,  $100\% \pm 0\%$ , and 2/100 Hz,  $97\% \pm 1.97\%$ ;  $P < 0.01$ , one-way ANOVA; Fig. 5E).

These results suggest that conduction failure occurs when PES is continuously applied at 100 Hz, and PES at alternating frequency between 2 Hz and 100 Hz (2/100 Hz) for 3 s each improves the situation (details in Fig. S2).

### PES at Frequencies from 100 to 1000 Hz Delivered to the Receptive Fields of Afferent Fibers

The discharges evoked in A $\beta$  and A $\delta$  fibers in response to high-frequency stimulation were in various forms – irregular, proportional, burst, and sporadic (Fig. S3)

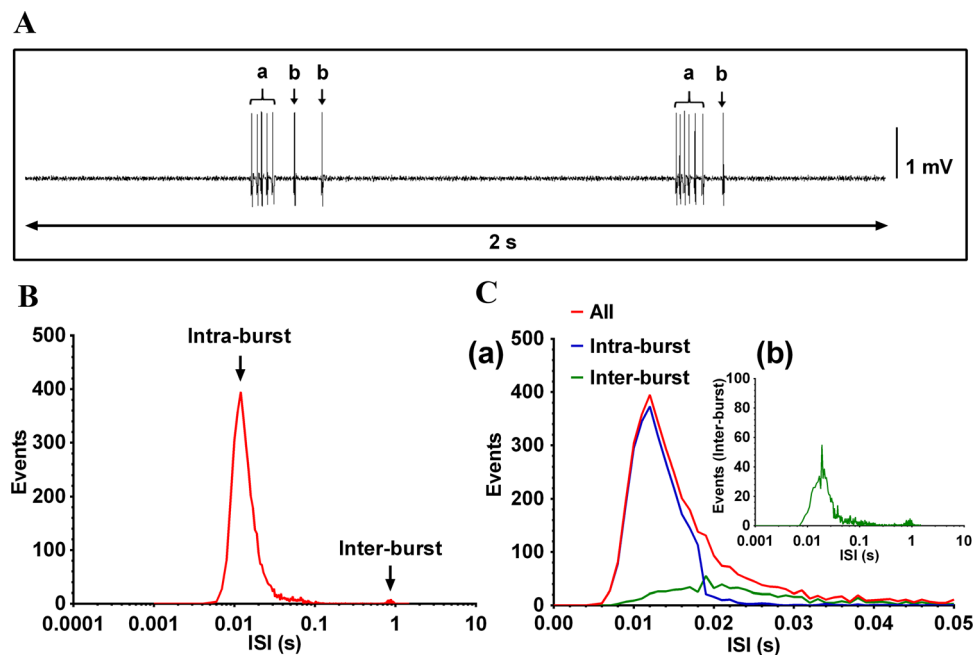
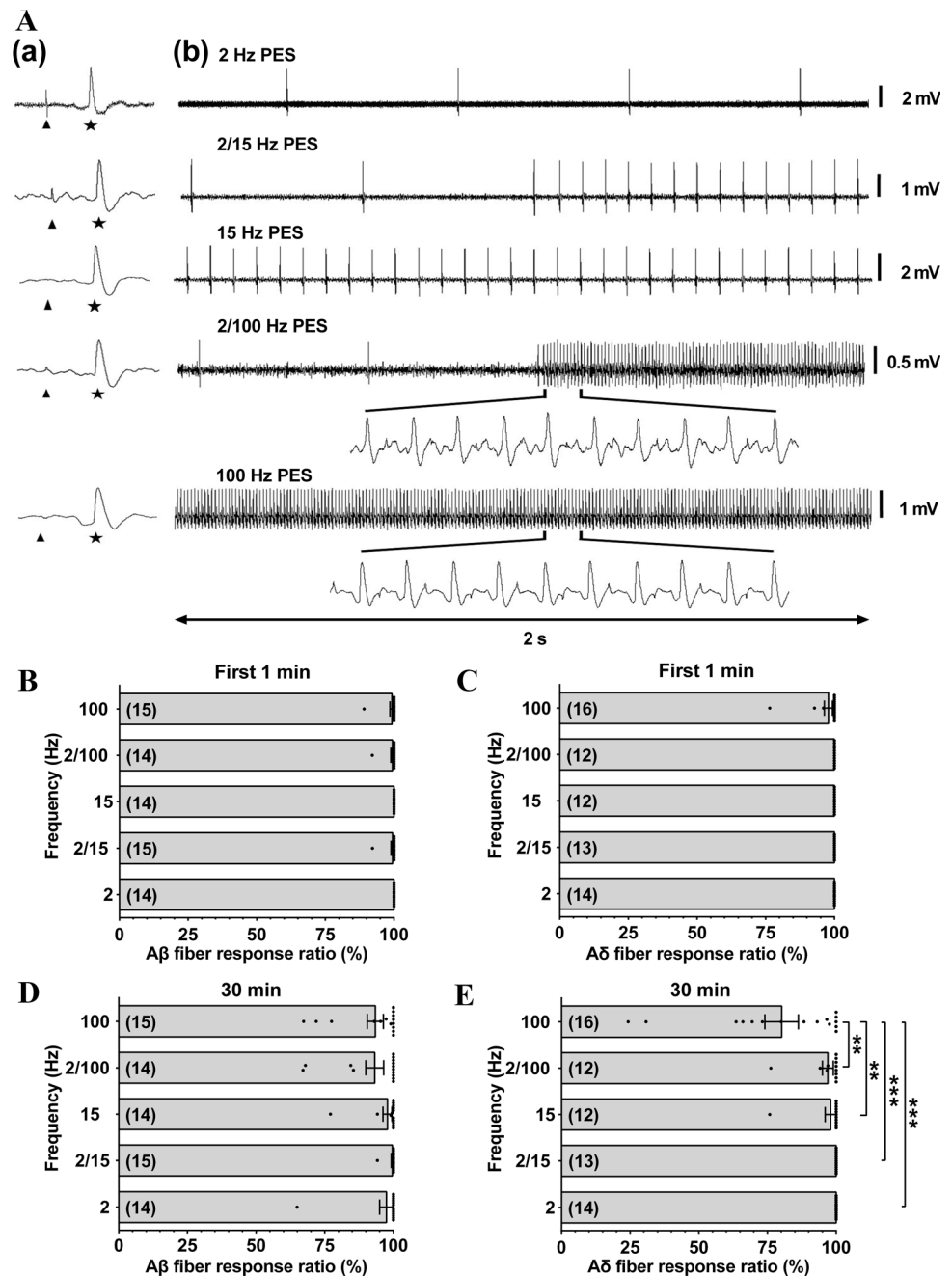


**Fig. 4** ISI distribution of evoked discharges of PAN fibers in response to MAc at once per second. **A** Examples of burst firing (**a**) and sporadic firing (**b**) of evoked discharges. **B** Distribution of ISIs of evoked discharges in all 11 recorded burst-firing fibers in response to MAc at once per second. Note log scale on abscissa. **C** (**a**) Distribution of burst firing (intra-burst) and sporadic firing (inter-burst) of all 11 recorded burst-firing fibers according to the burst

criteria (maximum intra-burst ISI  $\leq 0.019$  s; minimum inter-burst ISI  $> 0.1$  s; and minimum number of spikes in a burst  $\geq 3$ ). The intra-burst ISI peak within a burst was  $\sim 0.012$  s (arrow) and the inter-burst ISI was  $\sim 1$  s (arrow). (**b**) Distribution of sporadic firing (inter-burst and intra-burst) of all 11 fibers. PAN, primary afferent nerve; MAc, manual acupuncture; ISI, inter-spike interval.

**Fig. 5** Spike traces and response ratios of single-unit afferent fibers in response to PES at optimal frequencies. **A** (a) Evoked discharges (stars) of A $\beta$  fibers (conduction velocities 31.06, 30.60, 30.00, 26.48, and 26.81 m/s) induced by negative square-wave pulses (width 100  $\mu$ s, 1.5 $\times$  threshold current, stimulus artifact indicated by arrow) at their receptive fields; and (b) examples of one-to-one responses of the fibers in (a). **B**, **C** No difference in the response ratios during the initial 60 s among the different frequency groups in A $\beta$  or A $\delta$  fibers in response to PES at the optimal frequencies. **D**, **E** A significantly lower response ratio is found only in A $\delta$  fibers at 100 Hz in response to 30 min PES. Digits in brackets are the numbers of recorded fibers. Data are expressed as the mean  $\pm$  SEM. **\*\*** $P < 0.01$  and **\*\*\*** $P < 0.001$ ; one-way ANOVA. PES, peripheral electrical stimulation.



### Changes in Response Ratio of Afferent Fibers with Increasing Frequency of PES (100 to 1000 Hz)

In these experiments, 32 A $\beta$  single-unit afferent fibers were recorded from 7 rats, and 30 A $\delta$  fibers were recorded from 11 rats. Each fiber received PES using at least one of the following randomly-selected frequencies: 100 Hz, 200 Hz, 300 Hz, 400 Hz, 500 Hz, 600 Hz, 700 Hz, 800 Hz, 900 Hz, and 1000 Hz. The corresponding numbers of A $\beta$  fibers were 17, 17, 17, 14, 15, 13, 14, 16, 14, and 12, and the numbers of A $\delta$  fibers were 18, 21, 14, 10, 14, 8, 12, 9, 13,

and 14. The response ratios of A $\beta$  and A $\delta$  fibers declined gradually with increasing frequency of PES above 100 Hz (Fig. 6A, B), reaching a plateau 20 s after PES started. The response ratios of A $\beta$  and A $\delta$  fibers in the last 10 s of 60-s stimulation at various frequencies were relatively stable and used for analysis. The response ratios of both A $\beta$  and A $\delta$  fibers dramatically deteriorated as the frequency of PES approached 1000 Hz. Furthermore, the response ratio in A $\delta$  fibers deteriorated more quickly than that in A $\beta$  fibers under the same experimental conditions ( $P < 0.001$ , repeated measures ANOVA; Fig. 6C).



### Changes in Frequency of Evoked Discharges of Afferent Fibers with Increasing Frequency of PES (100 Hz–1000 Hz)

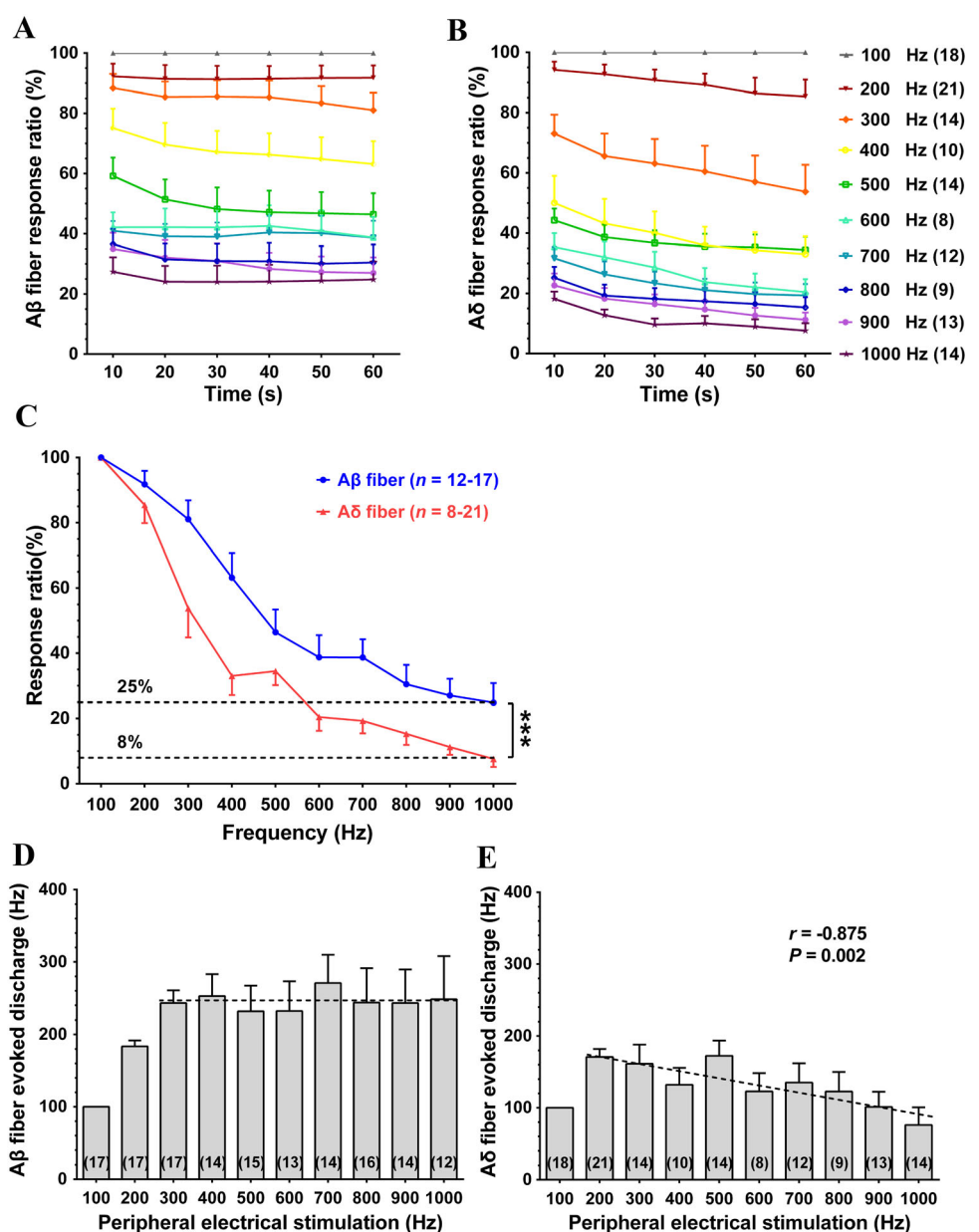
Changes in the frequency of evoked discharges in response to PES at given frequencies serve as another way to describe the frequency-conduction relationship in neurons. We found that the number of evoked discharges per second in Aβ fibers increased with an increase in the frequency of PES between 100 Hz and 300 Hz (Fig. 6D). However, the number of evoked discharges per second remained at 246 in Aβ fibers in spite of PES frequency further increasing from 300 to 1000 Hz.

A similar decrease in evoked discharges was found in Aδ fibers; the maximum number of evoked discharges per

second was <200 at 200-Hz PES. There was a steady decrease in the evoked discharges with an increase in the frequency; in fact, there was a significant negative correlation between the number of evoked discharges and the frequency of PES in the range of 200 Hz–1000 Hz ( $r = -0.875$ ,  $P = 0.002$ ; Fig. 6E).

These data demonstrate the limit of efficiency in PAN fibers in transmitting high-frequency signals. The response ratio decreases dramatically when the frequency of peripheral stimulation exceeds a certain level in term of the axon diameter and the refractory period of afferent nerve fibers. These PANs function as a frequency filter to prevent signals >300 Hz in Aβ fibers or 200 Hz in Aδ fibers from entering the CNS.

**Fig. 6** Response ratios and evoked discharge rates of Aβ and Aδ fibers in response to PES at various frequencies. **A**, **B** Response ratios of Aβ and Aδ fiber remain relatively stable after 20-s PES. **C** Response ratios gradually decrease with increasing stimulus frequency in both Aδ and Aβ fibers in the last 10 s of 60-s PES, and the curve is steeper in Aδ than in Aβ fibers (\*\* $P < 0.001$ , repeated measures ANOVA). **D**, **E** The discharge rates of Aβ fibers do not change in response to PES at 300 Hz–1000 Hz; and the discharge rates of Aδ fibers are negatively correlated with PES frequency at 200 Hz–1000 Hz. Digits in brackets are the numbers of recorded fibers. Data are expressed as the mean  $\pm$  SEM. PES, peripheral electrical stimulation.



## Discussion

We have demonstrated previously that at least some of the therapeutic effects of acupuncture such as pain relief are mediated by activity in the brain and spinal cord [15]. It is known that multiple types of PAN fibers are activated by peripheral stimulation. For example, Kagitani *et al.* reported that all the four populations of afferent fibers are activated by acupuncture and 5–7 spikes per second occur in A-fibers induced by manual twisting once per second [19]. This is in good agreement with our data. However, we suggest that the analgesic acupuncture signal from the periphery to the CNS appears to be mediated primarily by the large-diameter myelinated A $\beta$  and A $\delta$  fibers of PANs since the anti-nociceptive effect is lost after the afferents being blocked by local anesthetics [29] but not by capsaicin [2], which selectively blocks C-fibers.

Chang *et al.* also reported distinct and persistent burst discharges from pressing or manipulating needles in the receptive fields [3]. Our results showed that MAc induced four different patterns of evoked discharges in A $\beta$  and A $\delta$  fibers. They can be simplified into two categories: burst firing and sporadic firing. Burst firing was the dominant pattern of evoked discharges in MAc at a frequency of once per second, which induced  $\sim 6$  spikes per burst on average. The frequency of evoked intra-burst discharges was  $\sim 90$  Hz, which occurred mostly when the needle started moving from zero to the maximum angular velocity. Distortion of the nerve terminal near the needle is assumed to be responsible. The sporadic firing mainly consisted of tonic and irregular patterns; the ISIs varied dramatically. The average frequency of sporadic firing was  $\sim 2$  Hz, lower than in the burst firing (90 Hz). The two types of firing pattern in PANs can be viewed as two types of acupuncture signals: high frequency and low frequency signals.

To avoid inconsistent MAc, we used an EAc device that provided precise and reproducible rotation angle, rotation speed, and up-down movement. The data further showed that increasing the rotation angle from 90° to 360° did not further increase the number of evoked discharges per second. In contrast, there was a frequency-dependent increase in the evoked discharges when the twisting frequency was increased from one cycle per second to three cycles per second.

PES in the receptive field of the PANs mimics the EA effect. Different stimulus thresholds were found at different frequencies. For example, the threshold was lower at 2 Hz than at 100 Hz. This difference was most likely due to the greater pulse width used at 2 Hz (Fig. S4). A wider pulse was used in 2-Hz stimulation during the dense-disperse mode in order to deliver more energy per pulse to offset the

difference in the total energy delivered between low and high frequencies during a given period of time. Otherwise the sensation would be too weak during 2 Hz stimulation compared with the 100 Hz stimulation.

It is generally accepted that low- and high-frequency stimulation have distinct neural transmission pathways and activate different neurotransmitter/neuropeptide systems in different parts of the CNS resulting in different therapeutic effects [11, 32, 33, 38]. For example, we have previously demonstrated that 2-Hz EA stimulates the release of beta endorphin in the brain which acts on mu and delta opioid receptors [13, 15]. In contrast, 100-Hz EA stimulates the release of spinal dynorphin which acts on kappa opioid receptors [15]. Based on these findings, an EA stimulator capable of delivering dense-disperse mode between 2 Hz and 100 Hz, for 3 s each, appears to have a better pain-relieving effect [6]. It is interesting that MAc also produced low- (2 Hz) and high (90 Hz)-frequency discharges in PANs. These two frequencies are almost the same as those recommended for use in electroacupuncture (2 Hz and 100 Hz) [11]. From the above results it is clear that the MAc signal is transmitted into the CNS by PAN fibers with a 100% transmission response ratio. In addition, the 2 Hz and 100 Hz alternating stimulation pattern recommended for use in EA appears to mimic the signal produced by MAc in PANs (2 Hz and 90 Hz).

The therapeutic effects of acupuncture for many disorders appear to be frequency-dependent. For example, low-frequency EA has been shown to be better than high-frequency in improving ovary function in reproductive medicine [34]. Low-frequency is also better at improving behavioral symptoms in autistic children [35], while high-frequency is more effective than low-frequency for the treatment of myospasm and arthritic pain [24]. Therefore, the appropriate acupuncture manipulation style in MAc or frequency parameters in EA would be selected for a better therapeutic effect for a particular disorder. Based on our data, an acupuncturist requiring more high-frequency or burst signals in MAc would choose twisting with short strokes and frequent turning back and forth rather than long strokes, since burst firing mostly occurs at the beginning of each twist.

One of the purposes of the present study was to provide information to facilitate the establishment of a limit on the maximum output frequency for EA stimulators to be published by the International Organization for Standardization. The results showed that the EA signal is in the physiological range when reaching the dorsal horn after the high-frequency signal had been filtered by the PANs. Some EA stimulators on the market deliver very high frequencies which are certainly beyond the physiological range of signals that a neuron can transmit. Very high frequencies should not be recommended since they do not have

therapeutic advantages and may expose the patients to unnecessary risks associated with high energy output. Therefore, we examined the transmission capacity of PAN fibers over a wide range of frequencies of PES and concluded that the A $\beta$  and A $\delta$  fibers in PANs transmit the EA-like signal faithfully when the frequency is <100 Hz. The response ratio was reduced in a frequency-dependent manner when PES was between 100 Hz and 300 Hz. The induced discharges in A $\beta$ -fibers stabilized at 246 per second even when the PES frequency was raised to 1000 Hz. However, the number of evoked discharges gradually decreased from a peak when PES was between 200 Hz and 1000 Hz in A $\delta$  fibers. The dropping of evoked spikes (i.e. the response ratios of the PANs) at higher frequencies is presumably due to the diameter and the refractory period of the PAN axons, because the smaller the diameter of the afferent nerve fibers, the slower conduction velocity and the longer the refractory period of excitation, and therefore the lower the frequency of response to peripheral stimuli such as EA and PES. Other factors such as the presence or absence of myelin sheath around the fibers also have influence on the response ratios of the PANs to the PES frequency. This phenomenon has also been reported by others [10, 23, 30, 31] including Gasser and Grundfest who found the refractory period to be  $\sim 0.4$  ms in rabbit alpha fibers, imposing a maximum frequency of evoked discharge to be  $\sim 250$  Hz [9]. Furthermore, the transmission efficiency of both A $\beta$  and A $\delta$  fibers dropped further during prolonged stimulation at higher frequencies. Here, we found that the decrease in response ratio appeared to be reversible, suggesting that temporary intracellular imbalance of electrolytes or ions may be responsible [27]. Using the radiant heat/tail-flick latency method to measure changes in nociception threshold in rats, our previous studies have shown that EA stimulation at ST36 and SP6 at 2000 Hz has an anti-nociceptive effect [22] which can be partially reversed by a high dose of naloxone capable of blocking all opioid receptors ( $\mu$ ,  $\delta$ , and  $\kappa$ ). Our present findings suggest that the EA signal is in the physiological range when reaching the dorsal horn after high-frequency signals are filtered out by the PAN. However, our study also had limitations. We did not examine the evoked responses in different fiber types in the manual and emulated acupuncture experiments. It cannot be ruled out that different fibers respond differently, for example, bursting might be preferentially associated with A $\beta$  rather than A $\delta$  fibers. To our knowledge, the present study is the first to quantitatively describe the response ratio and the rate of evoked discharges in A $\beta$  and A $\delta$  fibers in response to PES at various frequencies. Unlike another study [30], the intensity of PES used in our study was double the activation threshold current of the afferent fibers, closer to that used in clinical practice. Furthermore,

a positive control (100-Hz PES) was included after each testing frequency to ensure that the fibers responded to PES normally with no shift in the baseline.

Although A $\beta$  and A $\delta$  fibers cannot follow very high frequency stimulation (>100 Hz), such stimulation may still have analgesic effects in terms of spinal cord stimulation. Future studies are encouraged to study acupuncture and single-unit recordings in animals with inflammatory pain or neuropathic pain.

## Conclusions

The present findings suggest the coexistence of high-frequency and low-frequency evoked firing and frequency-dependent responses occur in PANs following MAc and PES. A $\beta$  and A $\delta$  fibers may serve as filters to prevent very high frequency signals from entering the CNS. Therefore, EA therapy with frequencies >250 Hz appears to be ineffective at least for the purpose of pain relief.

**Acknowledgments** We wish to thank JY Wei of the University of California at Los Angeles and Zhi-Qi Zhao of Fudan University for their suggestions throughout the study. Special thanks go to Hua-Yuan Yang, Yi-Ming Zhang, and Gang Xu of Shanghai University of Traditional Chinese Medicine for their generosity in providing equipment for emulation acupuncture. In addition, we thank Xiao-Ping Kang, Yao Huang, Chang-Xi Xu, Zhi-Jun Lv, and Zhen-Chen Liu for their help with part of the data analysis. This work was supported by the National Key Research and Development Program of the Ministry of Science and Technology, China (2016YFC0105501, 2019YFC1712104 and 2016YFF0202802) and the National Natural Science Foundation of China (81974169, 81671085 and 61527815).

**Conflict of interest** The authors declare no conflicts of interest.

## References

1. Bäcker M, Hammes MG, Valet M, Deppe M, Conrad B, Tölle TR, *et al.* Different modes of manual acupuncture stimulation differentially modulate cerebral blood flow velocity, arterial blood pressure and heart rate in human subjects. *Neurosci Lett* 2002, 333: 203–206.
2. Bao H, Zhou Z, Yu Y, Han J. C fiber is not necessary in electroacupuncture analgesia, but necessary in diffuse noxious inhibitory controls (DNIC). *Zhen Ci Yan Jiu* 1991, 16: 120–124.
3. Chang SC, Wei JY, Mao CP. Deep innervation of sural nerve. *Brain Res* 1983, 279: 262–265.
4. Chang XB, Wang S, Meng ZH, Fan XN, Yang X, Shi XM. Study on acupuncture parameters impacting on the acupuncture effect using cluster analysis in a rat model with middle cerebral artery occlusion. *Chin J Integr Med* 2014, 20: 130–135.
5. Chen W, Chi YN, Kang XJ, Liu QY, Zhang HL, Li ZH, *et al.* Accumulation of Cav3.2 T-type calcium channels in the uninjured sural nerve contributes to neuropathic pain in rats with spared nerve injury. *Front Mol Neurosci* 2018, 11: 24.

6. Chen XH, Guo SF, Chang CG, Han JS. Optimal conditions for eliciting maximal electroacupuncture analgesia with dense-and-disperse mode stimulation. *Am J Acupunct* 1994, 22: 47–53.
7. Choi YJ, Lee JE, Moon WK, Cho SH. Does the effect of acupuncture depend on needling sensation and manipulation? *Complement Ther Med* 2013, 21: 207–214.
8. Fang JL, Krings T, Weidemann J, Meister IG, Thron A. Functional MRI in healthy subjects during acupuncture: different effects of needle rotation in real and false acupoints. *Neuroradiology* 2004, 46: 359–362.
9. Gasser HS, Grundfest H. Axon diameter in relation to the spike dimensions and the conduction velocity in mammalian A fibers. *Am J Physiol* 1939, 127: 393–414.
10. Gee MD, Lynn B, Cotsell B. Activity-dependent slowing of conduction velocity provides a method for identifying different functional classes of C-fibre in the rat saphenous nerve. *Neuroscience* 1996, 73: 667–675.
11. Han JS. Acupuncture: neuropeptide release produced by electrical stimulation of different frequencies. *Trends Neurosci* 2003, 26: 17–22.
12. Han JS. Acupuncture and endorphins. *Neurosci Lett* 2004, 361(1–3): 258–261.
13. Han JS, Sun SL. Differential release of enkephalin and dynorphin by low and high frequency electroacupuncture in the central nervous system. *Acupunct Sci Int* 1990, 1: 19–27.
14. Han JS, Terenius L. Neurochemical basis of acupuncture analgesia. *Annu Rev Pharmacol Toxicol* 1982, 22: 193–220.
15. Han JS, Wang Q. Mobilization of specific neuropeptides by peripheral stimulation of identified frequencies. *Physiology* 1992, 7: 176–180.
16. Hong S, Ding S, Wu F, Xi Q, Li Q, Liu Y, *et al.* Strong manual acupuncture manipulation could better inhibit spike frequency of the dorsal horn neurons in rats with acute visceral nociception. *Evid Based Complement and Alternat Med* 2015, 2015: 675437.
17. Hunt CC. Relation of function to diameter in afferent fibers of muscle nerves. *J Gen Physiol* 1954, 38: 117–131.
18. Jiang Y, Wang H, Liu Z, Dong Y, Dong Y, Xiang X, *et al.* Manipulation of and sustained effects on the human brain induced by different modalities of acupuncture: an fMRI study. *PLoS One* 2013, 8: e66815.
19. Kagitani F, Uchida S, Hotta H, Aikawa Y. Manual acupuncture needle stimulation of the rat hindlimb activates group I, II, III and IV single afferent nerve fiber in the dorsal spinal roots. *Jpn J Physiol* 2005, 55: 149–155.
20. Kim SA, Lee BH, Bae JH, Kim KJ, Steffensen SC, Ryu YH, *et al.* Peripheral afferent mechanisms underlying acupuncture inhibition of cocaine behavioral effects in rats. *PLoS One* 2013, 8: e81018.
21. Kress M, Koltzenburg M, Reeh PW, Handwerker HO. Responsiveness and functional attributes of electrically localized terminals of cutaneous C-fibers *in vivo* and *in vitro*. *J Neurophysiol* 1992, 68: 581–595.
22. Lin JG, Chen XH, Han JS. Antinociception produced by 2 and 5 KHz peripheral stimulation in the rat. *Int J Neurosci* 1992, 64: 15–22.
23. Littlefield PD, Vujanovic I, Mundi J, Matic AI, Richter CP. Laser stimulation of single auditory nerve fibers. *Laryngoscope* 2010, 120: 2071–2082.
24. Liu HX, Tian JB, Luo F, Jiang YH, Deng ZG, Xiong L, *et al.* Repeated 100 Hz TENS for the treatment of chronic inflammatory hyperalgesia and suppression of spinal release of substance P in monoarthritic rats. *Evid Based Complement Alternat Med* 2007, 4: 65–75.
25. Li WM, Chen YB, Wang XY. Characteristics of peripheral afferent nerve discharges evoked by manual acupuncture and electroacupuncture of “Zusanli” (ST 36) in rats. *Zhen Ci Yan Jiu* 2008, 33: 65–70.
26. Li X, Li Y, Chen J, Zhou D, Liu Y, Li Y, *et al.* The influence of skin microcirculation blood perfusion at zusanli acupoint by stimulating with lift-thrust reinforcing and reducing acupuncture manipulation methods on healthy adults. *Evid Based Complement and Alternat Med* 2013, 2013: 452697.
27. Lüscher C, Streit J, Lipp P, Lüscher HR. Action potential propagation through embryonic dorsal root ganglion cells in culture. II. Decrease of conduction reliability during repetitive stimulation. *J Neurophysiol* 1994, 72: 634–643.
28. Min S, Lee H, Kim SY, Park JY, Chae Y, Lee H, *et al.* Local changes in microcirculation and the analgesic effects of acupuncture: a laser doppler perfusion imaging study. *J Alternat Complement Med* 2015, 21: 46–52.
29. Research Group of Acupuncture Anesthesia, Peking Medical College. Effect of acupuncture on the pain threshold of human skin. *Chin Med J* 1973, 3: 151–157.
30. Tang JS, Shi WC, Hou ZL. Effect of electroacupuncture stimulation (EAS) of different frequencies on the excitability of fibers of various groups. *Zhen Ci Yan Jiu* 1987, 12: 68–72.
31. Torebjörk HE, Hallin RG. Responses in human A and C fibres to repeated electrical intradermal stimulation. *J Neurol Neurosurg Psychiatry* 1974, 37: 653–664.
32. Wang Q, Mao L, Han J. The arcuate nucleus of hypothalamus mediates low but not high frequency electroacupuncture analgesia in rats. *Brain Res* 1990, 513: 60–66.
33. Wang Q, Mao L, Han J. The role of parabrachial nucleus in high frequency electroacupuncture analgesia in rats. *Chin J Physiol Sci* 1991, 7: 363–367.
34. Zhang R, Feng XJ, Guan Q, Cui W, Zheng Y, Sun W, *et al.* Increase of success rate for women undergoing embryo transfer by transcutaneous electrical acupoint stimulation: a prospective randomized placebo-controlled study. *Fertil Steril* 2011, 96: 912–916.
35. Zhang R, Jia MX, Zhang JS, Xu XJ, Shou XJ, Zhang XT, *et al.* Transcutaneous electrical acupoint stimulation in children with autism and its impact on plasma levels of arginine-vasopressin and oxytocin: A prospective single-blinded controlled study. *Res Dev Disabil* 2012, 33: 1136–1146.
36. Zhou T, Wang J, Han CX, Torao I, Guo Y. Analysis of interspike interval of dorsal horn neurons evoked by different needle manipulations at ST36. *Acupunct Med* 2014, 32: 43–50.
37. Zhou W, Fu LW, Tjen-A-Looi SC, Li P, Longhurst JC. Afferent mechanisms underlying stimulation modality-related modulation of acupuncture-related cardiovascular responses. *J Appl Physiol* 2005, 98: 872–880.
38. Wang Y, Wang Y, Liu J, Wang M. Electroacupuncture alleviates motor symptoms and up-regulates vesicular glutamatergic transporter 1 expression in the subthalamic nucleus in a unilateral 6-hydroxydopamine-lesioned hemi-parkinsonian rat model. *Neurosci Bull* 2018, 34: 476–484.